Continuum-distorted-wave–final-state approximation in positron-hydrogenic atom (ion) collisions with positronium formation

O. A. Fojón and R. D. Rivarola
Instituto de Física Rosario, CONICET-UNR y Escuela de Ciencias Exactas y Naturales, Facultad de Ciencias Exactas, Ingeniería y Agrimensura, Avenida Pellegrini 250, 2000 Rosario, Argentina

R. Gayet
Centre de Physique Théorique et de Modélisations, CNRS Equipe de Recherche No. 1537, Université de Bordeaux I, Talence, France

J. Hanssen and P. A. Hervieux
Laboratoire de Physique Moléculaire et des Collisions, Institut de Physique Rue Arago, Téchnopôle 2000, Metz, France
3 November 1995; revised manuscript received 18 March 1996

We study theoretically the formation of positronium atoms through electron capture in collisions of positrons impacting on hydrogenlike targets such as He^+, Li^{2+}, and Be^{3+}. We obtain the scattering amplitude of the charge-exchange process by using a distorted-wave model derived from the first order of a Dodd and Greider's expansion. We compute differential and total cross sections by using a partial-wave technique. [S1050-2947(96)03808-5]

PACS number(s): 34.70.+e, 36.10.Dr

I. INTRODUCTION

Theoretical studies of positron-atom collisions [1–5] have been promoted in recent years due to the technological advances that made possible the obtainment of high-intensity positron beams. As a result of this progress, positronium total cross-section measurements were performed over an extended energetic domain although at intermediate and high impact energies the available data are still quite limited [6–9].

In this work, we study collisions of positrons impacting on hydrogenic targets in the ground state leading to the formation of positronium atoms also in the ground state. Gayet [10] applied successfully the Dodd and Greider formalism [11,12] to study the charge transfer in the proton-hydrogen collision deriving the continuum distorted wave approximation (CDW) [13] from the first order of the mentioned formalism.

Following Gayet's ideas, Mandal, Mandal, and Mukherjee [3] have used this formalism to study the positronium formation with neutral hydrogen targets. We generalize the model of Mandal, Mandal, and Mukherjee to the case of charged hydrogenic targets such as He^+, Li^{2+}, and Be^{3+} ions. We pay extreme attention to the correct asymptotic Coulomb conditions that require the residual interactions in the initial channel result short ranged. As in the model of Mandal, Mundal, and Mukherjee, an intermediate potential V_x related to the Coulomb continuum states of the positron and the electron in the field of the residual target is included in the final channel. As V_x is closely linked to the CDW approximation, we call our model continuum-distorted-wave–final-state (CDW–FS). The charged target introduces additional complications through the inclusion of a continuum state in the entry channel. We obtain with our CDW–FS model differential and total cross sections at different impact energies and for several targets. It is well established that the CDW approximation of Cheshire [13] contains second-order terms associated to the classical two-step Thomas' mechanism. It is expected that our model gives information on the existence of these processes in the case of positronium formation. We use atomic units unless otherwise specified.

II. THEORY

We consider the formation of positronium atoms in a collision of a positron e^+ with a monoelectronic (hydrogenlike) target T of nuclear charge Z_T at high impact energies. The reaction of interest may be written as

$$e^+ + (T + e^-) \rightarrow (e^+ + e^-) + T, \tag{1}$$

where pairs of parenthesis indicate bound states. The geometrical parameters of the collision are given in Fig. 1. $\mathbf{r}_\alpha$ indicates the position of e^+ with respect to the center-of-mass of the target. $\mathbf{r}_\beta$ gives the position of the target nucleus with respect to the center-of-mass of e^+ and e^-.

In the frame linked to the center-of-mass of the whole system, we may write the total Hamiltonian $\mathcal{H}$ as

$$\mathcal{H} = \mathcal{H}_\alpha + V_\alpha = \mathcal{H}_\beta + V_\beta, \tag{2}$$

where $\mathcal{H}_\alpha$ and $\mathcal{H}_\beta$ are the Hamiltonians of the entrance and exit channels α and β, respectively. V_α and V_β are the perturbations relevant to α and β, respectively. Channel Hamiltonians must be defined so that asymptotic Coulomb conditions are preserved. As the final channel is described in the same way as in the model of Mandal, Mundal, and Mukherjee [3], we only analyze in what follows the initial channel that must be treated in a different way because net charged fragments are involved. Therefore one may write in the entrance channel

$$\mathcal{H}_\alpha = H_\alpha + h_\alpha, \tag{3}$$

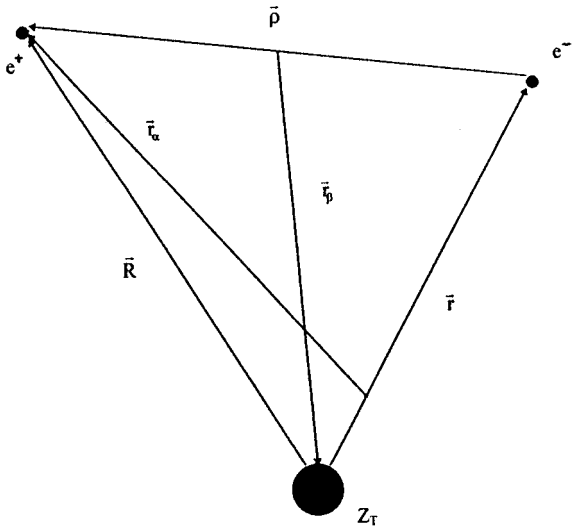

FIG. 1. Coordinates used in the text.

$$H_\alpha = -\frac{1}{2\mu_\alpha}\nabla^2_{\mathbf{r}_\alpha} + \frac{Z_T-1}{r_\alpha}, \tag{4}$$

$$h_\alpha = -\frac{1}{2m_\alpha}\nabla^2_{\mathbf{r}} - \frac{Z_T}{r}, \tag{5}$$

$$V_\alpha = \frac{Z_T}{R} - \frac{1}{\rho} - \frac{Z_T-1}{r_\alpha}, \tag{6}$$

where h_α is the Hamiltonian for the hydrogenlike target and H_α is the Hamiltonian for the evolution of the positron. The introduction of the Coulomb interaction $(Z_T-1)/r_\alpha$ in H_α preserves the required asymptotic conditions. The reduced masses that appear in expressions (4) and (5) are given by

$$\mu_\alpha = \frac{M_T+1}{M_T+2} \quad m_\alpha = \frac{M_T}{M_T+1}. \tag{7}$$

Let us introduce now $\mathbf{k}_\alpha$ and $\mathbf{k}_\beta$, the wave vectors for the reduced positron in the entrance channel and for the reduced positronium in the exit channel, respectively. So, the initial wave function (eigenvector of $\mathcal{H}_\alpha$) is given by

$$\Phi_\alpha = \varphi_i(\mathbf{r})\mathcal{F}^+_{\mathbf{k}_\alpha}(\mathbf{r}_\alpha). \tag{8}$$

The function $\mathcal{F}^+_{\mathbf{k}_\alpha}(\mathbf{r}_\alpha)$ introduced in Eq. (8) is an outgoing Coulomb continuum wave function representing the positron moving in the field of an effective ion of charge (Z_T-1), so that

$$H_\alpha \mathcal{F}^+_{\mathbf{k}_\alpha}(\mathbf{r}\alpha) = \frac{k^2_\alpha}{2\mu_\alpha}\mathcal{F}^+_{\mathbf{k}_\alpha}(\mathbf{r}_\alpha), \tag{9}$$

where

$$\mathcal{F}^+_{\mathbf{k}_\alpha}(\mathbf{r}_\alpha) = N^+_{\nu'_\alpha}\exp(\iota\mathbf{k}_\alpha\cdot\mathbf{r}_\alpha)\,{}_1F_1(-\iota\nu'_\alpha;1;\iota k_\alpha r_\alpha - \iota\mathbf{k}_\alpha\cdot\mathbf{r}_\alpha), \tag{10}$$

$$\nu'_\alpha = (Z_T-1)\frac{\mu_\alpha}{k_\alpha}, \tag{11}$$

$$N^+_{\nu'_\alpha} = \Gamma(1+\iota\nu'_\alpha)\exp\left(-\frac{\pi}{2}\nu'_\alpha\right), \tag{12}$$

We write the final wave function ξ^-_β in the form

$$\xi^-_\beta = \mathcal{L}^-_\beta(\boldsymbol{\rho},\mathbf{r}_\beta)\varphi_f(\boldsymbol{\rho}), \tag{13}$$

where [3]

$$\begin{aligned}\mathcal{L}^-_\beta = N^-_{\beta_+}N^-_{\beta_-}\exp\{\iota(\mathbf{k}_+\cdot\mathbf{r}_\alpha+\mathbf{k}_-\cdot\mathbf{r})\}\,{}_1F_1(\iota\beta_+;1;\\ -\iota\mathbf{k}_+\cdot\mathbf{r}_\alpha-\iota k_+ r_\alpha)\,{}_1F_1(-\iota\beta_-;1;\\ -\iota\mathbf{k}_-\cdot\mathbf{r}-\iota k_- r),\end{aligned} \tag{14}$$

with

$$N^-_{\beta_\pm} = \Gamma(1\mp\iota\beta_\pm)\exp\left(\mp\frac{\pi}{2}\beta_\pm\right) \quad \beta_\pm = \frac{Z_T\mu_\alpha}{k_\pm}. \tag{15}$$

The correct asymptotic behavior imposes to the vectors $\mathbf{k}_+$ and $\mathbf{k}_-$ and introduced in Eq. (14) the following conditions:

$$\lim_{z_\beta\to-\infty}(\mathbf{k}_-\cdot\mathbf{r}+\mathbf{k}_+\cdot\mathbf{r}_\alpha) = -\mathbf{k}_\beta\cdot\mathbf{r}_\beta, \tag{16}$$

$$\begin{aligned}\lim_{z_\beta\to-\infty}\exp\{\iota\beta_-\ln(\mathbf{k}_-\cdot\mathbf{r}+k_- r)-\iota\beta_+\ln(\mathbf{k}_+\cdot\mathbf{r}_\alpha+k_+ r_\alpha)\}\\ = e^{\iota\gamma},\end{aligned} \tag{17}$$

with γ a constant real number. Under the condition $M_T\gg1$, which in turn implies that $\mathbf{r}_\alpha\simeq\mathbf{R}$, the following equality must be verified:

$$\frac{k^2_\beta}{2\mu_\beta} \simeq \frac{k^2_+}{2\mu_\alpha} + \frac{k^2_-}{2m_\alpha}, \tag{18}$$

so that

$$\mathbf{k}_+ \simeq \mathbf{k}_- \simeq v_\beta = \frac{\mathbf{k}_\beta}{\mu_\beta} \tag{19}$$

and

$$\beta_+ \simeq \beta_- \simeq \beta = \frac{Z_T}{v_\beta}. \tag{20}$$

In this way, $\mathcal{L}^-_\beta$ may be interpreted as a product of positron-target nucleus and electron-target nucleus continuum wave functions.

Finally, we write the CDW–FS matrix element in its *prior* version

$$\begin{aligned}T^{-,\mathrm{CDW-FS}}_{\alpha\beta} = N^+_{\nu'_\alpha}N^{-*}_{\beta_+}N^{-*}_{\beta_-}\int d\mathbf{r}_\alpha d\mathbf{r}\,\exp\{\iota\mathbf{k}_\alpha\cdot\mathbf{r}_\alpha\\ +\iota\mathbf{k}_\beta\cdot\mathbf{r}_\beta\}\varphi^*_f(\rho)\left(\frac{1}{r_\alpha}-\frac{1}{\rho}\right)_1 F_1(-\iota\beta_+;1;\end{aligned}$$

$$\iota\mathbf{k}_+\cdot\mathbf{r}_\alpha+\iota k_+ r_\alpha)\,{}_1F_1(\iota\beta_-;1;\iota\mathbf{k}_-\cdot\mathbf{r}+\iota k_- r)\,\varphi_i(\mathbf{r})$$
$$\times\,{}_1F_1(-\iota\nu'_\alpha;1;\iota k_\alpha r_\alpha-\iota\mathbf{k}_\alpha\cdot\mathbf{r}_\alpha) \tag{21}$$

with the conditions given by Eqs. (19) and (20).

In the limit $M_T\to\infty$, expression (21) coincides with the *prior* version of the first order distorted wave Born (DWB1) matrix element given by Bransden, Joachain, and McCann [4] for the case of neutral hydrogen targets. It is clear that our CDW–FS model does not satisfy the time-reversal invariance. In this sense, it is an asymmetric theory that will differ from the one obtained with a *post* form of the T-matrix element where the initial bound state is distorted by a product of positron-target nucleus and positron-electron wave functions as is the case for neutral hydrogen targets [4,5]. However, as we are interested in the description of Thomas' double-scattering mechanisms in which after a first collision between positron and electron, one of them should scatter in the target nucleus field, we use in our work the *prior* version of the T-matrix element. In this way, both required continua are implicitly introduced by the distortion appearing in the final wave function. Moreover, the distortion comes from the use of the intermediate potential V_x introduced in the Dodd and Greider formalism. The result obtained by Mandal, Mundal, and Mukherjee [3] for the simpler case of neutral hydrogen targets may be obtained up to an irrelevant phase factor by making $\nu'_\alpha=0$ in our Eq. (21).

If no distortions are included in the final channel through the potential V_x, the Coulomb Born approximation (CBA) [14,15] is obtained, whose matrix element in its *prior* version is given by

$$T^{-,\mathrm{CBA}}_{\alpha\beta}=N^+_{\nu'_\alpha}\int d\mathbf{r}_\alpha d\mathbf{r}\,\exp\{\iota\mathbf{k}_\alpha\cdot\mathbf{r}_\alpha+\iota\mathbf{k}_\beta\cdot\mathbf{r}_\beta\}\varphi_f^*(\rho)$$
$$\times\left(\frac{1}{r_\alpha}-\frac{1}{\rho}\right)_1 F_1(-\iota\nu'_\alpha;1;\iota k_\alpha r_\alpha-\iota\mathbf{k}_\alpha\cdot\mathbf{r}_\alpha)\varphi_i(\mathbf{r}) \tag{22}$$

The projectile-target interaction in the initial channel is fully included in the nonperturbed Hamiltonian. The residual perturbations in this CBA model are short ranged. A similar model has been used to study electron capture by proton impact [16]. This CBA differs from the Coulomb projected Born approximation introduced by Geltman [17] where the initial channel is described by a Coulomb function associated with the projectile-residual target interaction. This leads to long-ranged residual perturbations in the corresponding matrix element. The CDW–FS model includes higher-order terms than the CBA one. The potential V_x ensures that no disconnected diagrams are present in the complete Dodd and Greider's series.

Finally, we obtain differential (DCS) and total (TCS) cross sections by using

$$d\sigma/d\Omega=\frac{1}{4\pi^2}\frac{k_\beta}{k_\alpha}\mu_\alpha\mu_\beta|T_{\alpha\beta}|^2 \tag{23}$$

and

$$\sigma=\int d\Omega(d\sigma/d\Omega), \tag{24}$$

respectively.

III. EVALUATION OF THE CDW–FS MATRIX ELEMENT

We have developed a partial-wave expansion technique to evaluate the *prior* CDW–FS matrix element. This method is useful at intermediate and not very high energies. In the following, we describe the technique.

For monoelectronic targets in the ground state, we have

$$\varphi_i(\mathbf{r})=R_{1s}(r)Y_{00}(\hat{r}), \tag{25}$$

$$R_{1s}(r)=2Z_T^{3/2}e^{-Z_T r}, \tag{26}$$

and for the ground state of the positronium atom

$$\varphi_f(\boldsymbol{\rho})=\widetilde{R}_{1s}(\rho)Y_{00}(\hat{\rho}), \tag{27}$$

$$\widetilde{R}_{1s}(\rho)=\frac{1}{\sqrt{2}}\,e^{-\rho/2}. \tag{28}$$

We indicate with $Y_{l,m}$ the spherical harmonics of order (l,m) and with $\hat{r}(\hat{\rho})$ the unity vector associated with the vector $\mathbf{r}(\boldsymbol{\rho})$.

By using the approximation $\mathbf{R}\simeq\mathbf{r}_\alpha$ valid if $M_T\gg1$, we now write the expression of the CDW–FS matrix element given by Eq. (21) in the form

$$T^{-,\mathrm{CDW-FS}}_{\alpha\beta}=\int d\mathbf{R}\;\mathcal{F}^{-}_{\mathbf{k}_+}{}^*(\mathbf{R})V_T(\mathbf{R})\mathcal{F}^{+}_{\mathbf{k}_\alpha}(\mathbf{R}), \tag{29}$$

where we have defined

$$V_T(\mathbf{R})=\int d\mathbf{r}\;\varphi_f^*(\boldsymbol{\rho})\mathcal{F}^{-}_{\mathbf{k}_-}{}^*(\mathbf{r})\left(\frac{1}{R}-\frac{1}{\rho}\right)\varphi_i(\mathbf{r}). \tag{30}$$

$\mathcal{F}^{+}_{\mathbf{k}_\alpha}$ is given by Eq. (10) and

$$\mathcal{F}^{-}_{\mathbf{k}_\pm}(\mathbf{R})=N^-_{\beta_\pm}\,\exp(\iota\mathbf{k}_\pm\cdot\mathbf{R})\,{}_1F_1(\pm\iota\beta_\pm;1;-\iota k_\pm R$$
$$-\iota\mathbf{k}_\pm\cdot\mathbf{R}), \tag{31}$$

$N^-_{\beta_\pm}$ being given by Eq. (15).

The well known partial-wave expansion of the Coulomb wave function $\mathcal{F}^{\pm}_{\mathbf{k}}$ is given by

$$\mathcal{F}^{\pm}_{\mathbf{K}}(r)=\sum_{l,m}4\pi(\iota)^l e^{\pm\iota\delta_l}\frac{1}{kr}F_l(kr)Y^*_{l,m}(\hat{k})Y_{l,m}(\hat{r}). \tag{32}$$

The summation index l runs from zero to infinity whereas m runs from $m=-l$ to $m=l$. The Coulomb radial function and phase shift are given by

$$F_l(kr)=\frac{1}{2(2l+1)!}\,|\Gamma(l+1+i\eta)|e^{-\eta\pi/2}(2kr)^{l+1}e^{-\iota kr}$$
$$\times\,{}_1F_1(l+1-i\eta,\;2l+2,\;2ikr) \tag{33}$$

and

$$\delta_l = \arg\Gamma(l+1+i\eta) \tag{34}$$

with η being the Sommerfeld parameter.

For the particular case of $\mathcal{F}^-_{\mathbf{k}_-}$, we have $\eta=-\beta_-$ and $\mathbf{k}=\mathbf{k}_-$. Inserting the expressions of φ_i and φ_f and Eq. (32) into expression (30) of V_T, we have

$$V_T(\mathbf{R}) = \sqrt{2}(Z_T)^{3/2}\sum_{l,m}\int d\hat{r}\; r^2 dr\; e^{-\rho/2}\left(\frac{1}{R}-\frac{1}{\rho}\right)e^{-Z_T r} \times(-\imath)^l e^{\imath\delta_l} Y_{l,m}(\hat{k}_-) Y^*_{l,m}(\hat{r})\,\frac{1}{k_- r}\,F_l(k_- r). \tag{35}$$

We now define the function $J(\mathbf{r},\mathbf{R})$ as

$$J(\mathbf{r},\mathbf{R}) = e^{-\rho/2}\left(\frac{1}{R}-\frac{1}{\rho}\right) = \sum_{l',m'}\frac{4\pi}{(2l'+1)}\,J_{l'}(r,R)Y^*_{l,m'}(\hat{R})Y_{l',m'}(\hat{r}), \tag{36}$$

with

$$J_{l'}(r,R) = \frac{1}{2}(2l'+1)\int_{-1}^{1} du\; e^{-\rho/2}\left(\frac{1}{R}-\frac{1}{\rho}\right)P_{l'}(u) \tag{37}$$

and

$$\rho = (r^2+R^2-2rRu)^{1/2}, \tag{38}$$

P_l indicates the Legendre polynomial of degree l.

By using Eq. (37), expression (35) reads

$$V_T(\mathbf{R}) = \frac{8\pi}{\sqrt{2}}(Z_T)^{3/2}\frac{1}{k_-}\sum_{l,m}\sum_{l',m'}(-\imath)^l e^{\imath\delta_l} Y_{l,m}(\hat{k}_-) \times Y^*_{l',m'}(\hat{R})\int d\hat{r}\; Y_{l',m'}(\hat{r})Y^*_{l,m}(\hat{r}) \times\int_0^\infty dr\; r J_{l'}(r,R)\,\frac{1}{(2l'+1)}\,e^{-Z_T r}F_l(k_- r). \tag{39}$$

Since

$$\int d\hat{r}\; Y_{l',m'}(\hat{r})Y^*_{l,m}(\hat{r}) = \delta_{ll'}\delta_{mm'}, \tag{40}$$

we finally obtain

$$V_T(\mathbf{R}) = \frac{8\pi}{\sqrt{2}}(Z_T)^{3/2}\frac{1}{k_-}\sum_{l,m}(-\imath)^l e^{\imath\delta_l}\nu_l(R)Y_{l,m}(\hat{k}_-) \times Y^*_{l,m}(\hat{R}), \tag{41}$$

with

$$\nu_l(R) = \int_0^\infty dr\; r e^{-Z_T r}F_l(k_- r)\widetilde{J}_l(r,R), \tag{42}$$

$$\widetilde{J}_l(r,R) = \frac{1}{(2l+1)}\,J_l(r,R), \tag{43}$$

ν_l being the radial part of the transition potential V_T.

In order to perform the partial-wave expansion of the matrix element (29), the Coulomb wave functions $\mathcal{F}^{-*}_{\mathbf{k}_+}$ and $\mathcal{F}^{+}_{\mathbf{k}_\alpha}$ are expanded in the same way as expression (32) with $\eta=\beta_+$, $\mathbf{k}=\mathbf{k}_+$ and $\eta=\nu'_\alpha$, $\mathbf{k}=\mathbf{k}_\alpha$, respectively.

By using expression (41) into (29), we obtain the partial-wave expansion of the CDW–FS matrix element

$$T^{-,\mathrm{CDW-FS}}_{\alpha\beta} = \frac{128\pi^3 Z_T^{3/2}}{\sqrt{2}k_- k_+ k_\alpha}\sum_{l,m}\sum_{l_i,m_i}\sum_{l_f,m_f}\imath^{l_i-l-l_f}e^{\imath(\delta_{l_i}+\delta_l+\delta_{l_f})} \times\int d\hat{R}\; Y_{l_i,m_i}(\hat{R})Y^*_{l,m}(\hat{R})Y^*_{l_f,m_f}(\hat{R})\int_0^\infty dR \times F_{l_i}(k_\alpha R)\,\nu_l(R)F_{l_f}(k_+R)Y^*_{l_i,m_i}(\hat{k}_\alpha)Y_{l,m}(\hat{k}_-) \times Y_{l_f,m_f}(\hat{k}_+). \tag{44}$$

Choosing now the z axis along the vector $\hat{k}_\alpha$, we obtain

$$Y_{l_i,m_i}(\hat{k}_\alpha) = \sqrt{(2l_i+1)/4\pi}\,\delta_{0m_i}, \tag{45}$$

and employing the following definitions and results:

$$\mathcal{R}^l_{l_i l_f} = \int_0^\infty dR\; F_{l_i}(k_\alpha R)\,\nu_l(R)F_{l_f}(k_+R), \tag{46}$$

$$\hat{l} = 2l+1, \tag{47}$$

$$\int d\hat{R}\; Y_{l_i,m_i}(\hat{R})Y^*_{l,m}(\hat{R})Y^*_{l_f,m_f}(\hat{R}) = (-1)^{m+m_f}\left[\frac{\hat{l}_i\hat{l}\hat{l}_f}{4\pi}\right]^{1/2}\begin{pmatrix} l_i & l & l_f\\ 0 & 0 & 0\end{pmatrix}\begin{pmatrix} l_i & l & l_f\\ 0 & -m & -m_f\end{pmatrix}, \tag{48}$$

we have

$$T^{-,\mathrm{CDW-FS}}_{\alpha\beta} = \frac{32\pi^2 Z_T^{3/2}}{\sqrt{2}k_- k_+ k_\alpha}\sum_{l_i}\sum_{l,m}\sum_{l_f}(\imath)^{l_i-l-l_f}e^{\imath(\delta_{l_i}+\delta_l+\delta_{l_f})} \times\hat{l}_i(\hat{l}\hat{l}_f)^{1/2}\begin{pmatrix} l_i & l & l_f\\ 0 & 0 & 0\end{pmatrix}\begin{pmatrix} l_i & l & l_f\\ 0 & -m & m\end{pmatrix} \times\mathcal{R}^l_{l_i l_f}Y_{l,m}(\hat{k}_-)Y_{l_f,-m}(\hat{k}_+), \tag{49}$$

where we have used the fact that Eq. (48) implies that $m_f=-m$.

We now make $\mathbf{k}_+\simeq\mathbf{k}_-\simeq\mathbf{v}_\beta$. Therefore

$$\hat{k}_+ = \hat{k}_- = \hat{k}_\beta. \tag{50}$$

By using the two following formulas:

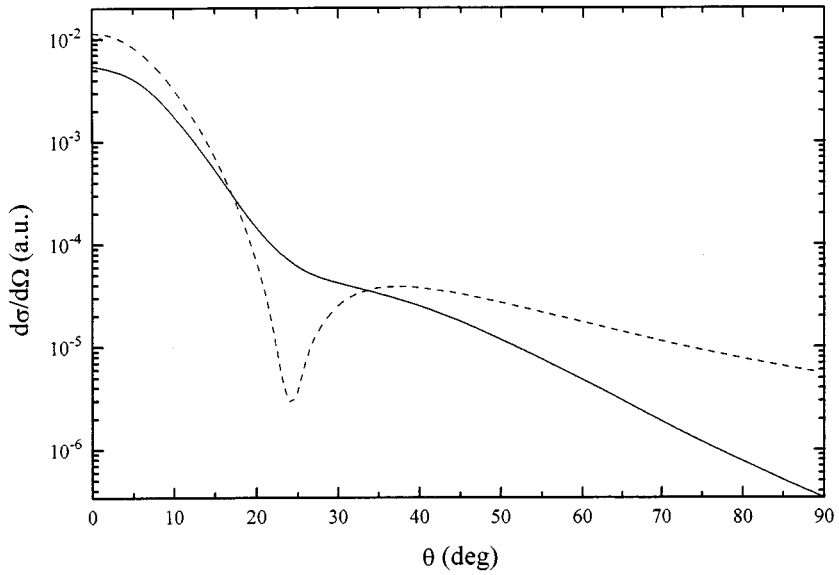

FIG. 2. CDW–FS (full line) and CBA (dashed line) differential cross sections for $e^+ + \mathrm{He}^+(1s) \rightarrow Ps(1s) + \mathrm{He}^{2+}$ at positron impact energy $E_i = 500$ eV.

$$Y_{l,m}(\hat{k}_\beta) Y_{l_f,-m}(\hat{k}_\beta) = \sum_L \left[\frac{\hat{l}\hat{l}_f\hat{L}}{4\pi}\right]^{1/2} \begin{pmatrix} l & l_f & L \\ 0 & 0 & 0 \end{pmatrix} \times \begin{pmatrix} l & l_f & L \\ m & -m & 0 \end{pmatrix} Y_{L,0}(\hat{k}_\beta) \quad (51)$$

and

$$\sum_m \begin{pmatrix} l_i & l & l_f \\ 0 & -m & m \end{pmatrix} \begin{pmatrix} l & l_f & L \\ m & -m & 0 \end{pmatrix} = \frac{1}{2l_i+1}\,\delta_{L l_i}, \quad (52)$$

with $l_i + l + l_f = 2p$ and $p \in N$, we obtain the simplified expression of the CDW–FS matrix element

$$T^{-,\mathrm{CDW-FS}}_{\alpha\beta} = \frac{8\pi Z_T^{3/2}}{\sqrt{2} v_\beta^2 k_\alpha} \sum_{l_i} \sum_{l} \sum_{l_f} \iota^{l_i - l - l_f} e^{\iota(\delta_{l_i} + \delta_l + \delta_{l_f})} \times \hat{l}_i \hat{l} \hat{l}_f \begin{pmatrix} l_i & l & l_f \\ 0 & 0 & 0 \end{pmatrix} \mathcal{R}^l_{l_i l_f} P_{l_i}(\cos\theta_\beta) \quad (53)$$

with $\mathcal{R}^l_{l_i l_f}$ given by Eq. (46).

IV. RESULTS

We have obtained differential and total cross sections with our *prior* CDW–FS model for several hydrogenic targets and energies. As a check to our calculations, we have compared our predictions with other existing theoretical results. In particular we have reproduced the differential cross sections for hydrogen targets given by Mandal, Mandal, and Mukherjee [3] at $E_i = 200$ eV (positron impact energy). In addition, our results for hydrogen targets at $E_i = 100$ eV and 500 eV are in agreement with the DWB1 results of Bransden, Joachain, and McCann [4] in its *prior* version. The DWB1 results exhibit a marked *post-prior* discrepancy. The difference between *post* and *prior* DWB1 differential cross sections is more pronounced at large scattering angles. In the total cross sections, the gap between both versions decreases as the impact energy increases. As discrepancies of this kind are expected in our model, our *prior* CDW–FS-results may differ considerably from the respective *post* results (not computed in this work) particularly for the lower energies and the above mentioned angular domain.

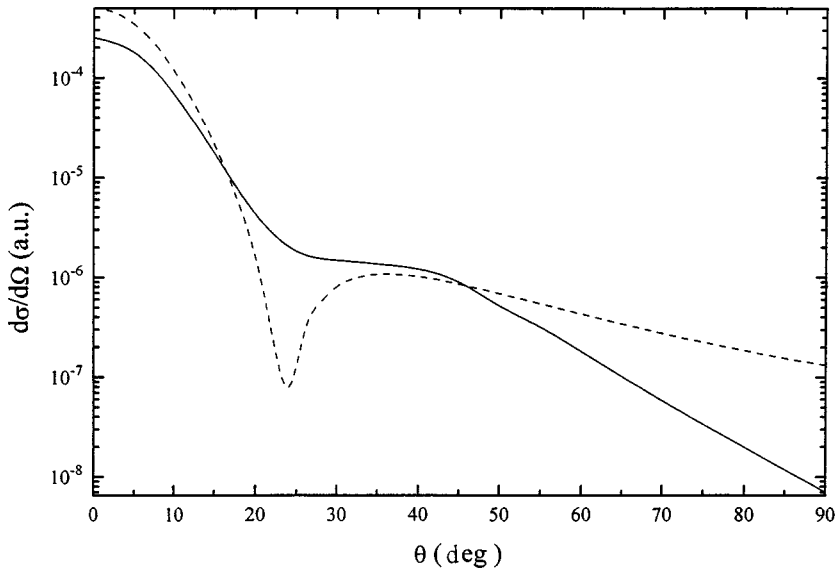

FIG. 3. Same as Fig. 2 but at positron impact energy $E_i = 1000$ eV.

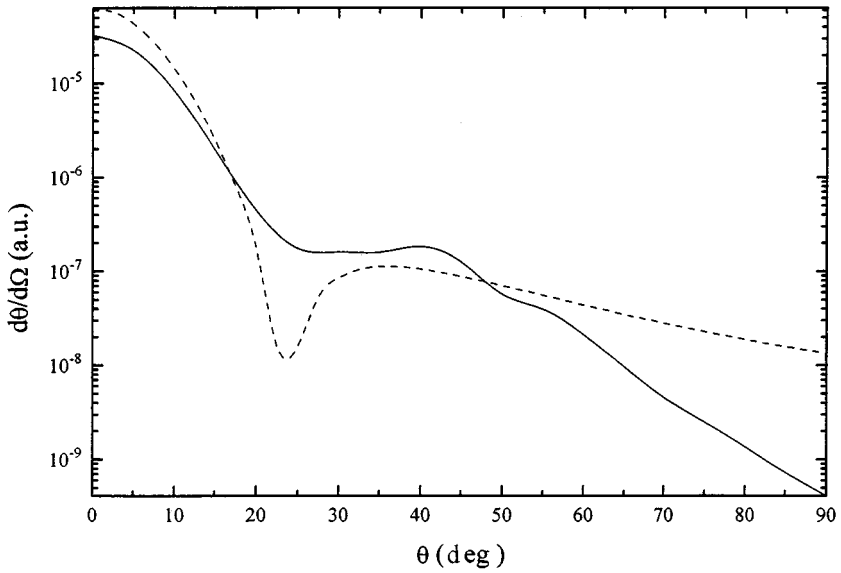

FIG. 4. Same as Fig. 2 but at positron impact energy $E_i=1500$ eV.

A. Differential cross sections

In Figs. 2, 3, 4, and 5 we introduce our results of differential cross sections for He^+ targets at impact energies of 500 eV, 1 keV, 1.5 keV, and 2 keV, respectively. We compare in each figure the predictions of our CDW–FS and CBA models. In general, CDW–FS and CBA DCS differ considerably in all the angular domain. In particular, for large angle values, i.e., around 90°, they differ approximately by an order of magnitude. At small angles, i.e., near the zero angular region, the difference is lesser but still important. For example, at zero degrees the CBA DCS are approximately twice as big as the CDW–FS DCS. Moreover, the CBA DCS exhibits a pronounced dip around 25°. This well-known dip [4] comes from the cancellation of the contributions corresponding to the attractive and repulsive parts of the residual perturbation. On the contrary, the CDW–FS DCS do not present this dip. Moreover, as the energy increases structures appear in the CDW–FS DCS. At $E_i=1$ keV, a flat protuberance develops around 35° while at $E_i=2$ keV a sharper peak is located around 40° along with a less prominent peak around 55°. It is well established in the case of heavy projectiles that the CDW model includes higher-order terms of the Coulomb potential and is able to describe the Thomas peak in the DCS. The observed peak at 40° could be associated with the existence of Thomas' two-step collision mechanisms in the process of positronium formation. In the case of positrons as projectiles, two different two-step classical processes (hereafter denoted A and B) could be realized. Both A and B predict a critical dispersion angle of $\theta_c=45°$ for high-energy positrons. In process A, in the first step the positron collides with the electron (considered as a free electron) and the positron is dispersed θ_c. In the second step, the electron hits the target nucleus and emerges with the same angle θ_c and velocity as the positron and capture can take place easily. In process B, the roles of the positron and the electron are interchanged. In the first step, the positron collides with the electron and the electron is dispersed θ_c. The positron itself hits the target nucleus and emerges with the same angle θ_c and velocity as the electron and capture occurs. Shakeshaft and Wadhera [1] have predicted interferences between the

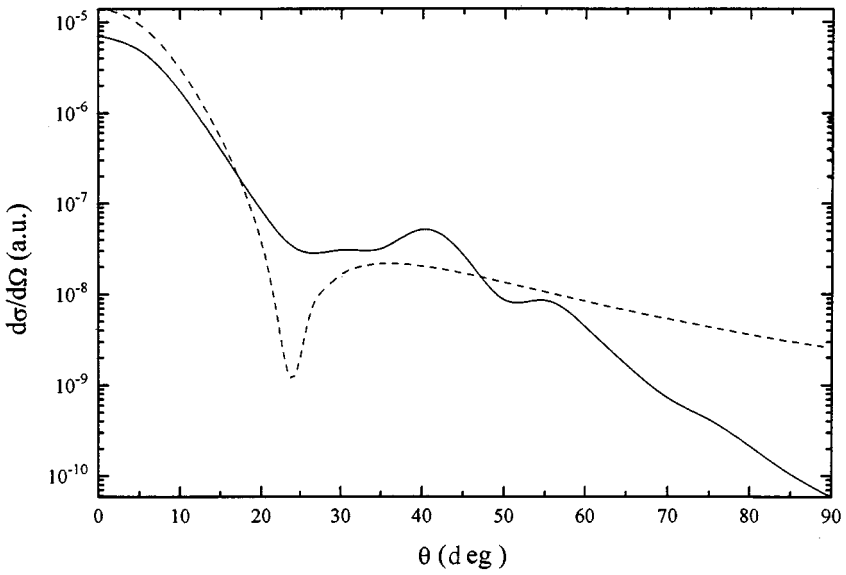

FIG. 5. Same as Fig. 2 but at positron impact energy $E_i=2000$ eV.

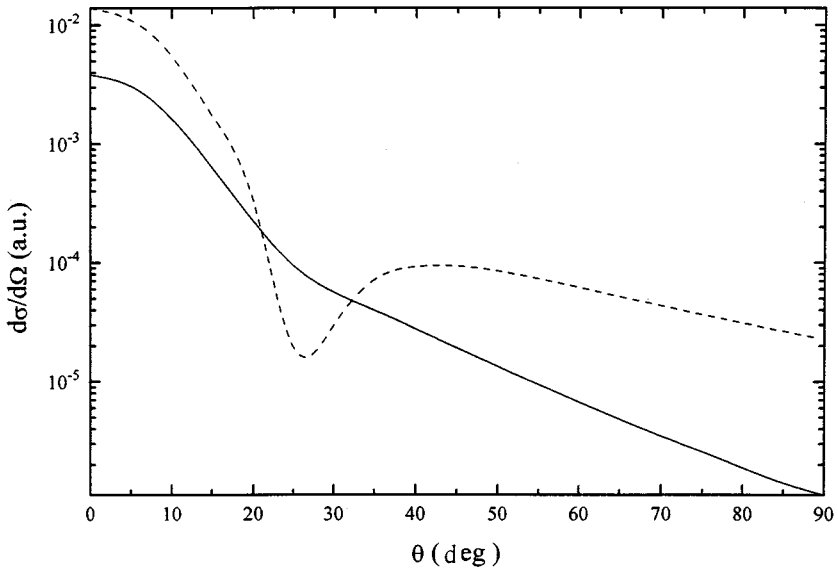

FIG. 6. CDW–FS (full line) and CBA (dashed line) differential cross sections for $e^+ + Li^{2+}(1s) \rightarrow Ps(1s) + Li^{3+}$ at positron impact energy $E_i = 500$ eV.

amplitudes associated with the classical processes A and B. The interferences are originated by the fact that the positron and the electron have the same mass but opposite charges. In particular, for the capture to the K shell of positronium atoms from the K shell of hydrogenic atoms a destructive interference is expected. Exact second-order Born calculations confirm this destructive effect but only for the imaginary part of the amplitude [18].

In Figs. 6 and 7 we show our results of CDW–FS differential cross sections for Li^{2+} and Be^{3+} targets at an impact energy of 500 eV. We also include in each figure the predictions of our CBA model. We analyze now the DCS at $E_i = 500$ eV for $Z_T = 2$, 3, and 4. At this energy, the CDW–FS DCS are lower than the CBA ones both in the small (around 0°) and in the large (around 90°) angle region. As the charge of the target increases this difference between the CDW–FS and CBA DCS increases. This is a measure of the importance of the final channel distortion appearing in the CDW–FS model. Around 0°, the CDW–FS DCS decrease monotonously as the charge of the target increases. On the other hand, in the same angular region the CBA DCS of Li^{2+} are slightly higher than the ones of He^+ whereas the Be^{3+} target exhibits the lowest DCS of all them.

B. Total cross sections

We have obtained CBA and CDW–FS TCS for He^+ targets at several impact energies. The results introduced in Table I give an estimation of the influence on TCS of the distortions appearing in the exit channel. At all the energies shown, the CBA TCS are greater than the CDW–FS TCS by a factor of approximately 1.8 except for the lowest energy. This fact could be understood recalling the above-mentioned behavior of the DCS near the zero angular region and the fact that at the energies considered the biggest contribution to the total cross sections comes from the small angular values. In particular, the peak at 40° in the DCS for He^+ at $E_i = 2$ keV contributes little to the total cross section. At higher impact velocities, the peak could be expected to become more and more pronounced with an angular width of

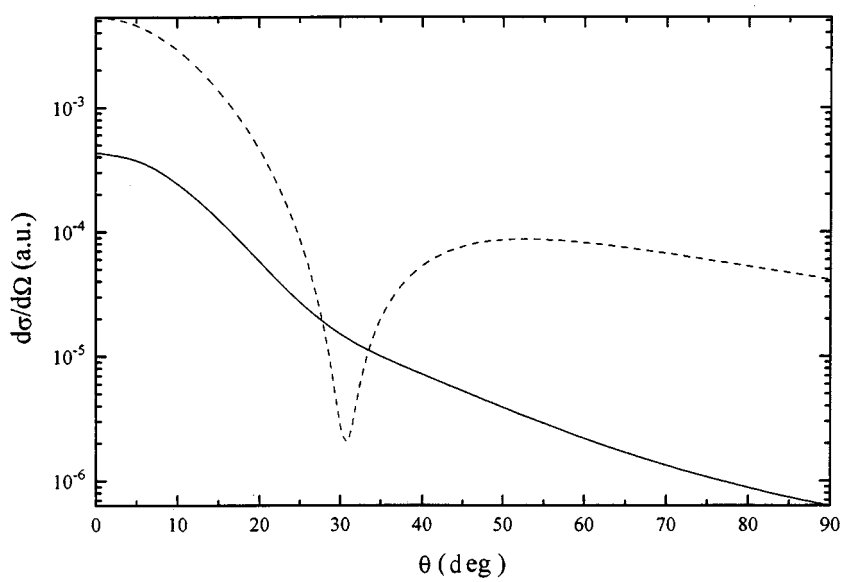

FIG. 7. CDW–FS (full line) and CBA (dashed line) differential cross sections for $e^+ + Be^{3+}(1s) \rightarrow Ps(1s) + Be^{4+}$ at positron impact energy $E_i = 500$ eV.

TABLE I. CBA and CDW-FS total cross sections for positronium formation with He^+ targets.

Energy (keV)	CBA (a.u.)	CDW-FS (a.u.)
0.25	1.5 [−2]	5.7 [−3]
0.50	9.4 [−4]	5.0 [−4]
0.75	1.5 [−4]	9.0 [−5]
1.00	3.5 [−5]	2.0 [−5]
1.25	1.1 [−5]	6.6 [−6]
1.50	4.3 [−6]	2.5 [−6]
2.00	9.4 [−7]	5.3 [−7]

order (Z_T/v_α). Therefore its contribution to the total cross section could be more important. Unfortunately, our calculation scheme exhibits practical limitations: as the energy increases the summation over the partial-wave index l to achieve convergence also increases. The method becomes a high-computer-time-consuming technique preventing us from introducing in this work DCS at very high impact energies.

V. CONCLUSIONS

We have introduced a distorted-wave model derived from the first order of a Dodd and Greider's expansion to study positronium formation with hydrogenic targets. Extreme attention is devoted to defining the corresponding channel perturbations so that asymptotic Coulomb conditions are preserved. The model includes distortions corresponding to continuum intermediate states associated with the Coulomb electron- and positron-target nucleus interactions in the final channel. The model shows evidence of the Thomas' two-step collision mechanisms involved in the reactions through the characteristic Thomas peak in the differential cross sections.

ACKNOWLEDGMENTS

The authors would like to thank the C.N.U.S.C. (Centre National Universitaire Sud de Calcul) for providing free computer time. One of us (O.A.F.) also gratefully acknowledges support from the University of Metz through collaboration with the University of Rosario.

[1] R. Shakeshaft and J. M. Wadhera, Phys. Rev. A **22**, 968 (1980).
[2] N. C. Deb, J. H. McGuire, and N. C. Sil, Phys. Rev. A **36**, 3707 (1987).
[3] C. R. Mandal, Mita Mandal, and S. C. Mukherjee, Phys. Rev. A **44**, 2968 (1991).
[4] B. H. Bransden, C. J. Joachain, and J. F. McCann, J. Phys. B **25**, 4965 (1992).
[5] B. H. Bransden and J. C. Noble, Adv. At. Mol. Opt. Phys. **32**, 19 (1994).
[6] L. Diana, P. Coleman, D. Brooks, P. Pendleton, and D. Norman, Phys. Rev. A **34**, 2731 (1986).
[7] D. Fromme, G. Kruse, W. Raith, and G. Sinapius, Phys. Rev. Lett. **57**, 3031 (1986).
[8] W. Sperber, D. Becker, K. G. Lynn, W. Raith, A. Schwab, G. Sinapius, G. Spicher, and M. Weber, Phys. Rev. Lett. **25**, 3690 (1992).
[9] M. Overton, R. J. Mills, and P. G. Coleman, J. Phys. B **26**, 3951 (1993).
[10] R. Gayet, J. Phys. B **5**, 483 (1972).
[11] K. R. Greider and L. D. Dodd, Phys. Rev. **146**, 671 (1966).
[12] L. D. Dodd and K. R. Greider, Phys. Rev. **146**, 675 (1966).
[13] I. M. Cheshire, Proc. Phys. Soc. **84**, 64 (1964).
[14] O. A. Fojón, R. Gayet, J. Hanssen, and R. D. Rivarola, Phys. Scr. **51**, 204 (1994).
[15] O. A. Fojón, Ph.D. thesis, Universidad Nacional de Rosario, 1994 (unpublished).
[16] S. Mukherjee, N. C. Sil, and D. Basu, J. Phys. B **12**, 1259 (1979).
[17] S. Geltman, J. Phys. B **4**, 1288 (1971).
[18] A. Igarashi and N. Toshima, Phys. Rev. A **47**, 2386 (1993).